

Table 1 Properties of the eddy core and its parent waters

	Return Atlantic water*, P1	Surface water†, P2	Mixture, 64% P1 + 36% P2	Eddy core‡
Salinity (p.s.u.)	34.894	34.810	34.864	34.872
Oxygen ($\mu\text{mol kg}^{-1}$)	320.5	358.7	334.2	329.7
CFC-11 (pmol kg^{-1})	4.63	7.00	5.48	5.74
CFC-12 (pmol kg^{-1})	2.22	3.34	2.62	2.69
SF ₆ (fmol l^{-1})	0.78	1.61	1.08	1.17
Potential temperature (°C)	-0.47	-1.55† - 1.8§	-0.86	-0.99§
			-0.95	

Water mass characteristics observed at various locations and times.
 * 74° 15' N, 6° W, 500 m depth, November 1996.
 † 75° N, 2° W, 10 m depth, May 1997.
 ‡ 75° N, 0° E, average of 300–900 m depth, May 1997.
 § Lowest temperature observed in March 1997 during winter cooling nearer the time of convection.

at the rim of the gyre, where the parent originating from return Atlantic water and that coming from inside-gyre surface waters, meet and mix. Because these coherent eddies are stable for ~1 year, they may also precondition water masses for convective activity in the following winter season. They could then form foci to concentrate further convection^{4,11,12} after erosion of the layer of less dense water that caps the core during the summer.

On the basis of float data only, we have direct evidence for about eight such eddies during ESOP-2. This probably underestimates the true number, because almost every float we released that strayed into the rim region of the Greenland gyre in 1997 became entrained in an anticyclonic eddy. When these eddies eventually decay, they presumably release their core water at mid-depths in the Greenland Sea, ventilating the intermediate water. Each eddy core has a volume ~50 km³. Comparing the volume of water in eight eddy cores to a total volume involved in convection of (2–4) × 10¹² m³ during 1996–97, a figure we have previously calculated from analysis of the tracer release experiment⁷, suggests a contribution of 10–20% to the total amount of convection from the eddies. However, only a small proportion—less than 10% of the total amount of water involved in convection—penetrated to around 1,000 m or deeper, most being confined to the upper ~500 m. Thus the eddies made a significant contribution to the total volume of deep convection—and dominated the water injected to substantial depth—in the Greenland Sea in 1996–97. Greenland Arctic Intermediate Water is thought to contribute to the overflows leading into the North Atlantic deep water, and the eddies thus provide a pathway for ventilation of the deep North Atlantic. Long-lived submesoscale anticyclonic vortices have also been observed in the Labrador Sea^{13,14} (another site known for deep ocean convection), indicating that such vortices may be ubiquitous features of deep ocean convection.

Received 19 October 2001; accepted 1 February 2002.

- Rudels, B., Quadfasel, D., Friedrich, H. & Houssais, M. N. Greenland Sea convection in the winter of 1987–1988. *J. Geophys. Res.* **94**, 3223–3227 (1989).
- Schott, F., Visbeck, M. & Fischer, J. Observations of vertical currents and convection in the central Greenland Sea during the winter of 1988–1989. *J. Geophys. Res.* **98**, 14401–14421 (1993).
- Morawitz, W. M. L., Sutton, P. J., Worcester, P. F. & Cornuelle, B. D. Three-dimensional observations of a deep convective chimney in the Greenland Sea during winter 1988/1989. *J. Phys. Oceanogr.* **26**, 2316–2343 (1996).
- Lherminier, P., Gascard, J.-C. & Quadfasel, D. The Greenland Sea in winter 1993 and 1994: Preconditioning for deep convection. *Deep Sea Res.* **46**, 1199–1235 (1999).
- McWilliams, J. C. Vortex generation through balanced adjustment. *J. Phys. Oceanogr.* **18**, 1178–1192 (1988).
- Marshall, J. & Schott, F. Open-ocean convection: observations, theory and models. *Rev. Geophys.* **37**, 1–64 (1999).
- Watson, A. J. *et al.* Mixing and convection in the Greenland sea from a tracer-release experiment. *Nature* **401**, 902–904 (1999).
- Gill, A. E. Homogeneous intrusions in a rotating stratified fluid. *J. Fluid Mech.* **103**, 275–295 (1981).
- Hedstrom, K. & Armi, L. An experimental study of homogeneous lenses in a stratified rotating fluid. *J. Fluid Mech.* **191**, 535–556 (1988).
- Roach, A. T., Aagaard, K. & Carsey, F. Coupled ice-ocean variability in the Greenland Sea. *Atmos. Ocean* **31**, 319–337 (1993).

- Legg, S., McWilliams, J. & Gao, J. Localisation of deep ocean convection by a mesoscale eddy. *J. Phys. Oceanogr.* **28**, 944–970 (1998).
- Straneo, F. & Kawase, M. Comparisons of localized convection due to localized forcing and to preconditioning. *J. Phys. Oceanogr.* **29**, 55–68 (1999).
- Gascard, J.-C. & Clarke, R. A. The formation of Labrador Sea Water. Part 2: mesoscale and smaller-scale processes. *J. Phys. Oceanogr.* **13**, 1779–1797 (1983).
- Lilly, J. M. & Rhines, P. B. Coherent eddies in the Labrador Sea observed from a mooring. *J. Phys. Oceanogr.* (special issue) (in the press).

Acknowledgements

We thank the staff and crew of RV *Håkon Mosby*, RV *Johan Hjort* and RRS *James Clark Ross* for their support. The main support for this work was from the programmes of the EU: European sub-polar ocean project (ESOP), Tracer and Circulation in the Nordic Seas Region (TRACTOR) and Monitoring the Atlantic Inflow toward the Arctic (MAIA). Additional support from the following national agencies was also important: IFRT (France), NERC (UK). ESOP required the involvement of a large number of individuals. We thank E. Jansen, coordinator of ESOP 2 and F. Rey for leading the RV *Johan Hjort* cruise; E. Fogelqvist, T. Tanhua, D. Wallace, C. Rouault and A. Lourencep for their contributions to the tracers and floats programmes respectively. NCEP-NCAR re-analysis data were provided through the NOAA Climate Diagnostics Center.

Competing interests statement

The authors declare that they have no competing financial interests.

Correspondence and requests for materials should be addressed to J.-C.G. (e-mail: gascard@lodyc.jussieu.fr).

Fin development in a cartilaginous fish and the origin of vertebrate limbs

Mikiko Tanaka*, Andrea Münsterberg*†, W. Gary Anderson‡, Alan R. Prescott§, Neil Hazon‡ & Cheryll Tickle*

* Division of Cell and Developmental Biology, § Division of Cell Biology and Immunology, Wellcome Trust Biocentre, University of Dundee, Dow Street, Dundee DD1 5EH, UK

‡ School of Biology, Division of Environmental and Evolutionary Biology, Gatty Marine Lab, University of St Andrews, St Andrews, Fife, KY16 8LB, UK

Recent fossil finds and experimental analysis of chick and mouse embryos highlighted the lateral fin fold theory, which suggests that two pairs of limbs in tetrapods evolved by subdivision of an elongated single fin¹. Here we examine fin development in embryos of the primitive cartilaginous fish, *Scyliorhinus canicula* (dogfish) using scanning electron microscopy and investigate expression of genes known to be involved in limb positioning, identity and patterning in higher vertebrates. Although we did not detect lateral fin folds in dogfish embryos, *Engrailed-1* expression suggests that the body is compartmentalized dorso-ventrally. Furthermore, specification of limb identity occurs through the *Tbx4* and *Tbx5* genes, as in higher vertebrates. In contrast, unlike higher vertebrates, we did not detect *Shh* transcripts in dogfish fin-buds, although *dHand* (a gene involved in establishing *Shh*) is expressed. In *S. canicula*, the main fin axis seems to lie parallel to the body axis. ‘Freeing’ fins from the body axis and establishing a separate ‘limb’ axis has been proposed to be a crucial step in evolution of tetrapod limbs^{2,3}. We suggest that *Shh* plays a critical role in this process.

The continuous fin fold theory was once considered to be ‘more an established fact than a theory’³ but was subsequently questioned because of inconsistencies in the fossil record and in the embryology of cartilaginous fish⁴. Recently discovered fossils of the earliest-

† Present address: School of Biological Sciences, University of East Anglia, Norwich, NR4 7TJ, UK.

known Cambrian vertebrates, however, seem to have had lateral ribbon-shaped fins⁵, and recent analysis of muscle formation in dogfish has shown uniform budding from somites in both limb and inter-limb regions⁶. The embryos of some primitive cartilaginous fish have been reported to have lateral fin folds⁷.

We therefore re-examined *Scyliohinus canicula* dogfish embryos from pre-fin-bud to fin-bud stages using scanning electron microscopy. In pre-fin-bud embryos (stage 22; ref. 8), no signs of lateral ridges could be detected (Fig. 1a). By stage 24 (about 3 days later), small shelf-like buds (pectoral fin buds) project out of the body wall just ventral to somites 5–13 (Fig. 1b). These buds are rimmed distally by a raised structure, the apical fold, and have discrete edges both anteriorly and posteriorly with no sign of continuation of the ‘shelf’ posteriorly along the flank. A thickening which will develop into pelvic fin buds is detected ventral to somites 27–36 (arrows; Fig. 1b). In later-stage embryos (stage 27, about 10–12 days older), pelvic fin buds (opposite somites 27–36) are present in addition to pectoral fin buds. Both types of bud are semicircular flaps rimmed with well defined apical folds. In between the buds, the body wall is quite smooth (Fig. 1c). Thus, we did not detect lateral folds in *S. canicula* embryos.

In chick embryos, the body ectoderm is compartmentalized with respect to the dorso-ventral axis in both limb-forming and flank regions⁹. This compartmentalization serves to position limbs laterally, because the apical ectodermal ridge, the thickened epithelium that mediates limb-bud outgrowth, arises at the compartment boundary. *Engrailed-1* expression is restricted to the ventral compartment of the body ectoderm of both chick and mouse embryos at pre-limb-bud stages and then in the ventral ectoderm and the ventral apical ridge of limb buds^{9,10}. To gain insight into ectoderm

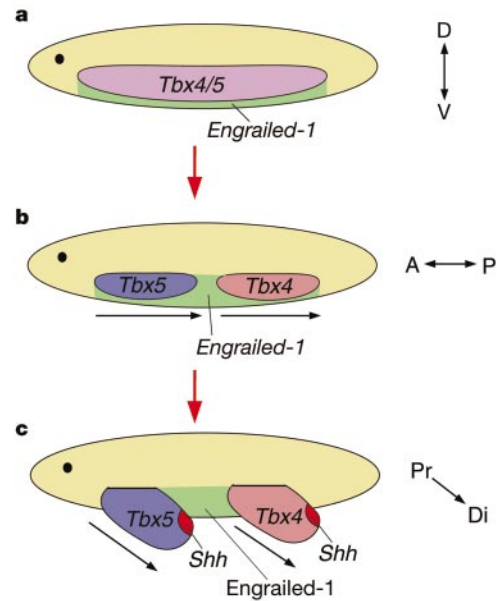


Figure 2 Model for evolution of vertebrate paired appendages. **a**, Hypothetical ancestral vertebrate with lateral fin folds, expressing *Tbx4/5*, positioned at the *Engrailed-1* expression boundary. **b**, *Tbx4/5* cluster duplication took place before the ancestor of cartilaginous fishes (or in that lineage) and inter-limb formation was suppressed. *Tbx5* and *Tbx4* are expressed in the pectoral and pelvic fins, respectively. **c**, Following the acquisition of *Shh* expression, the main axes of paired fins are freed from the body wall and establish the proximo-distal axes of the appendages. D, dorsal; V, ventral; A, anterior; P, posterior; Pr, proximal; Di, distal.

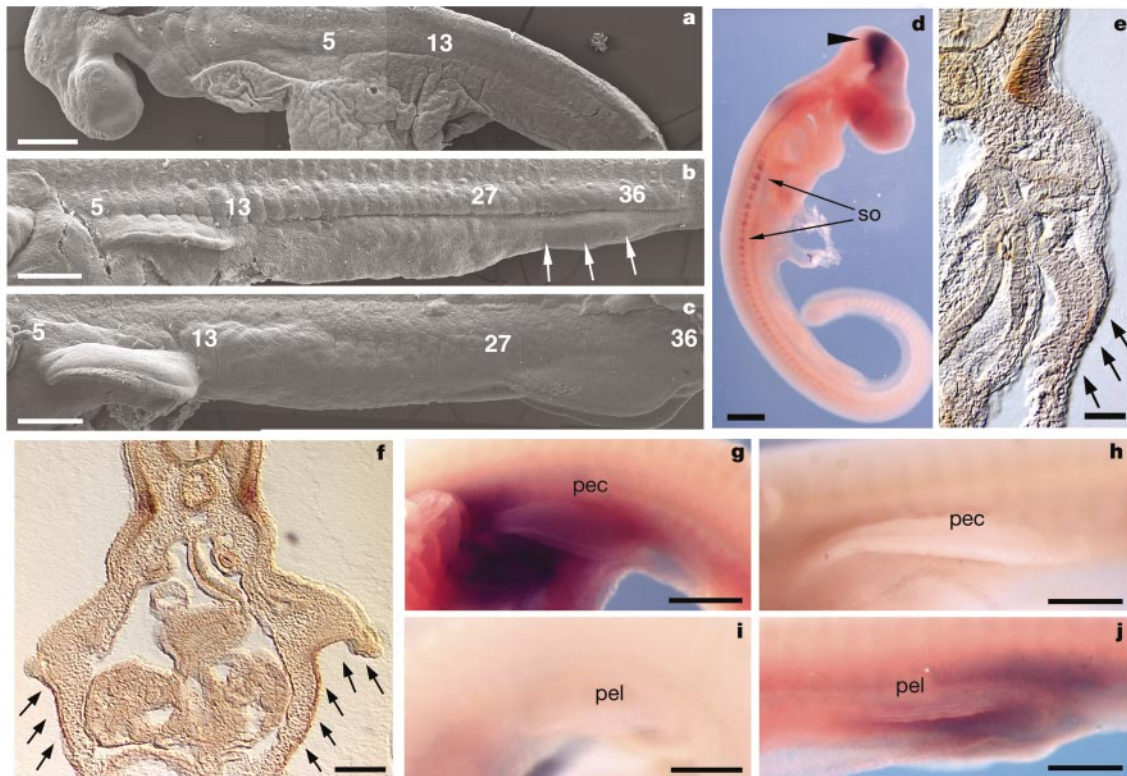


Figure 1 Scanning electron micrographs of *S. canicula* embryos. **a**, Stage 22; **b**, stage 24; and **c**, stage 27. **a–c**, Whole embryos. Pectoral and pelvic fins develop opposite somites 5–13 and 27–36 (arrows in **b**). Scale bars, 1 mm. **d**, Expression pattern of *ScEngrailed-1* in *S. canicula* embryos at stage 23. *ScEngrailed-1* expression is observed in the border of mesencephalon and metencephalon (arrowhead) and somites (arrows). Scale bar, 1 mm. **e**, **f**, Cross-sections of stage 23 and 26 embryos at pectoral fin-bud

level. *ScEngrailed-1* expression in presumptive fin buds region and fin buds indicated by arrows. Scale bars, 300 μ m in **e**, 500 μ m in **f**. **g–j**, *ScTbx4* and *ScTbx5* genes expression pattern in paired appendages in *S. canicula*. **g**, **i**, *ScTbx5* expression at stage 28. **g**, Pectoral fin. **i**, Pelvic fin. **h**, **j**, *ScTbx4* expression at stage 28. **h**, Pectoral fin. **j**, Pelvic fin. so, somite; pec, pectoral fin; pel, pelvic fin. Scale bars, 1 mm.

compartmentalization and whether fin buds of *S. canicula* arise at an ectodermal boundary of *Engrailed-1* expression, we isolated complementary DNA fragments of *ScEngrailed-1* and carried out whole-mount *in situ* hybridization on dogfish embryos. At both pre-fin (stage 23; Fig. 1d) and fin-bud stages, *ScEngrailed-1* transcripts were clearly seen at the border of the mesencephalon and metencephalon and in the somites. When these whole mounts were sectioned, *ScEngrailed-1* was seen to be expressed in the ventral ectoderm of the body of dogfish embryos both in the presumptive pectoral fin-bud region (stage 23 embryo; Fig. 1e) and in the pectoral fin buds themselves (stage 26 embryo; Fig. 1f). At the later stage, it was clear that, in the pectoral fin, the boundary between *ScEngrailed-1*-expressing ectoderm and non-*ScEngrailed-1*-expressing ectoderm lies at the mid-point of the apical fold, thus respecting the same boundary as *Engrailed-1* expression in chick and mouse limb buds. Thus, the pattern of *Engrailed-1* expression in *S. canicula* in relation to fin development suggests that the body of the dogfish is compartmentalized as in higher vertebrates. The mechanism that determines the dorso-ventral position of tetrapod limbs appears to be an ancient feature of the gnathostome body plan and could form the basis for a lateral fin fold in an ancestral vertebrate (Fig. 2a).

According to fin fold theory, two pairs of tetrapod limbs evolved by subdivision of a single lateral fin. In contrast, other recent ideas suggest that an ancestral vertebrate had a single pair of fins; either posterior¹¹ or anterior¹². In tetrapods and teleosts, the identity of each pair of appendages is determined by expression of T-box genes *Tbx5* and *Tbx4*, which are expressed in the anterior and posterior appendages, respectively¹³. In contrast, the cephalochordate *Amphioxus* has only one such gene, *AmphiTbx4/5* (ref. 14), although its expression pattern has not been reported. *Tbx4* and *Tbx5* genes in tetrapods are thought to have arisen by duplication of

this single ancestral gene. Therefore, we analysed the T-box gene complement in dogfish by employing polymerase chain reaction after reverse transcription of RNA (RT-PCR), using two sets of degenerate oligonucleotide primers. With each set of primers we obtained distinct PCR products, showing that the dogfish has both *Tbx4* and *Tbx5* genes. The deduced amino-acid sequences of *S. canicula Tbx4* and *Tbx5* T-box regions, aligned with those of zebrafish, chick, human homologues and the T-box region of *AmphiTbx4/5* are shown in Supplementary Information. The T-box region alignment provides further evidence that *ScTbx4* and *ScTbx5* belong to *Tbx4* and *Tbx5* subfamilies respectively. Skate embryos may also have a *Tbx5* gene¹³. In stage 28 dogfish embryos, *ScTbx5* expression was observed in pectoral fin buds (Fig. 1g), dorsal eye and heart, but not in pelvic fin buds (Fig. 1i). On the other hand, *ScTbx4* expression was not detected in pectoral fin buds (Fig. 1h), but was seen in pelvic fin buds (Fig. 1j). These results show that a *Tbx4/5* gene cluster duplication occurred before the origin of cartilaginous fish (Fig. 2b). Furthermore, as in tetrapods and teleosts, *Tbx5* and *Tbx4* are expressed in the anterior and posterior appendages, respectively.

An important recent finding with respect to the fin fold theory is that the inter-limb region in tetrapods has the potential to form limbs. Balinsky first discovered this in newts¹⁵ but limb-forming potential has now been described in both chick and mouse embryos^{16,17}. This remarkable property is associated with the potential of flank cells to form a polarizing region¹⁷. The polarizing region is the major limb 'organizer' and consists of mesenchyme at the posterior limb bud margin that expresses *Shh*¹⁸. We isolated an *ScShh* fragment using degenerate PCR and used this fragment to examine the *ScShh* expression pattern in stage 27 (Fig. 3a–c) and 28 (not shown) dogfish embryos. *ScShh* expression was observed in the floor plate, the notochord (Fig. 3b), the branchial arches (Fig. 3c),

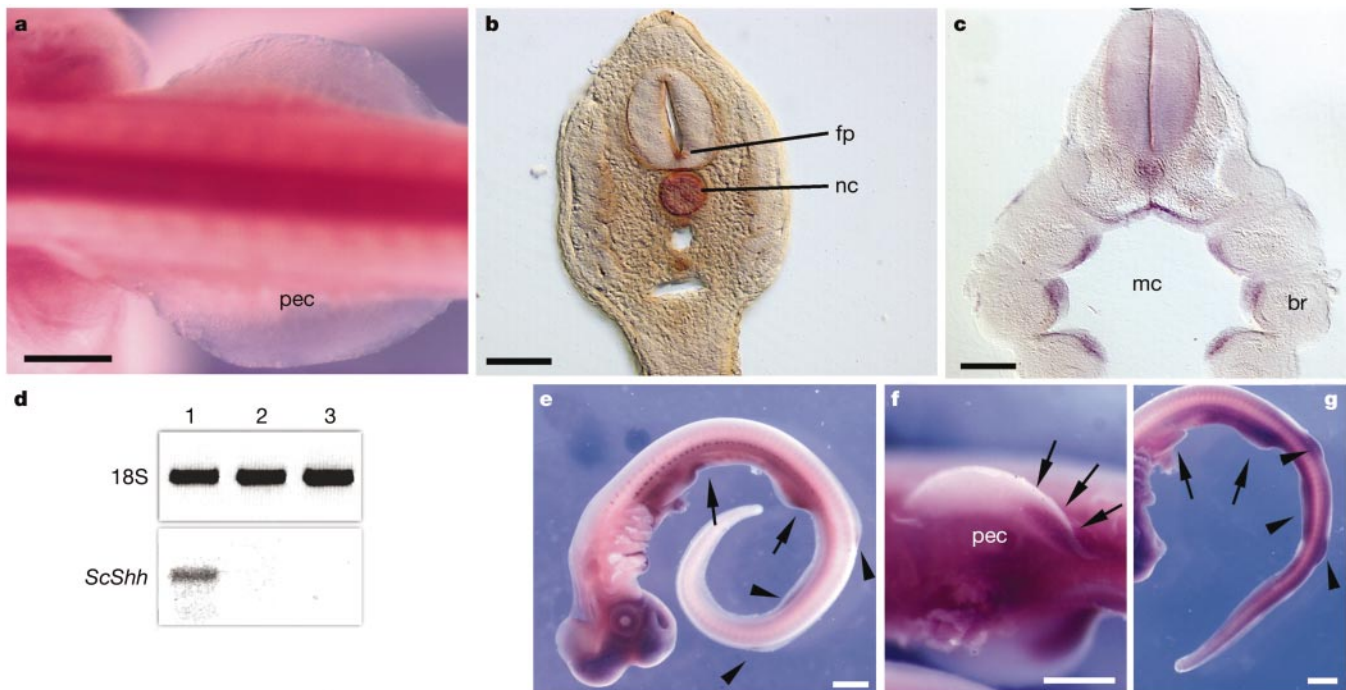


Figure 3 Gene expression patterns of stage 27–28 *S. canicula* embryos. **a–c**, Expression pattern of *ScShh* in stage 27 *S. canicula* embryos. *ScShh* is expressed in the floor plate, the notochord and the branchial arches (**b** and **c**), but not in the pectoral fin bud (**a**). Scale bars, 500 μm. **d**, *ScShh* expression of the stage 27 embryo was analysed by RT-PCR. *ScShh* expression was observed from body tissue (lane 1), but not from either pectoral (lane 2) nor pelvic fin-bud tissue (lane 3). 18S rRNA expression is shown as

an internal control. **e, f**, Expression pattern of *ScdHand* in stage 27 *S. canicula* embryo. *ScdHand* expression was observed in the posterior part of paired fin buds (arrows) and the dorsal and anal fin buds (arrowheads). Scale bars, 1 mm. **g**, Expression pattern of *ScBmp4* in stage 28 *S. canicula* embryo. *ScBmp4* expression was observed throughout paired fin buds (arrows) and dorsal and anal fin buds (arrowheads). pec, pectoral fin; fp, floor plate; nc, notochord; mc, mouth cavity; br, branchial arch. Scale bar, 1 mm.

the brain and the optic vesicle, but surprisingly we could not detect *Shh* expression in either pectoral (Fig. 3a) or pelvic fin buds. We extended the length of the *ScShh* probe using another set of primers, but even with this longer probe we were unable to detect a signal in fin buds. We further attempted to detect *ScShh* transcripts in stage 27 and 28 embryos by RT-PCR but although we were able to detect *ScShh* in the body, *ScShh* was not detected in either pectoral or pelvic fin buds (Fig. 3d). In zebrafish (*Danio rerio*), another member of the hedgehog gene family, *Tiggy-winkle hedgehog* (*Twhh*), has been reported¹⁹. It seems unlikely that the *Shh* we have isolated is *Twhh*

because *Twhh* is expressed only in the floorplate in zebrafish embryos¹⁹ and *ScShh* transcripts were observed in both the floorplate and the notochord in *S. canicula* embryos (Fig. 3b). Thus it appears that *Shh* must be expressed at very low levels, if at all, in the fin buds of dogfish embryos.

In higher vertebrates, genes that are involved in regulation of *Shh* expression (for example *dHand*²⁰) and that are targets of *Shh* signalling (for example, *Bmp4*; ref. 21) have been identified. We cloned these two genes from dogfish by degenerate PCR and examined their expression patterns. *ScdHand* transcripts were found in the same regions as in higher vertebrates, including the heart, the head and the posterior part of the fin buds where the polarizing region normally develops (Fig. 3e and f). In addition, *ScdHand* was detected at the posterior margins of the dorsal and anal fin buds (Fig. 3e). In higher vertebrates, *Bmp4* transcripts are abundant in anterior mesenchyme and expression is negatively regulated by *Shh*²¹. In dogfish fin buds, *ScBmp4* transcripts were detected throughout the fin bud (Fig. 3g), as might be predicted if *ScShh* expression is absent.

Our inability to detect *Shh* expression in dogfish fin buds was at first surprising. It could be that the acquisition of *Shh* expression in appendages was of primary importance for evolution of the distal regions. However, another possibility is that *Shh* could play a role in the 'freeing' of fins and the establishment of a proximo-distal limb axis (Fig. 2c). In *S. canicula*, as in many other cartilaginous fish, the metapterygium—the main long bone of the fin—develops parallel to the main body axis, in the proximal part of the fin bud next to the body wall (Fig. 4A). One hypothesis, which is still controversial, is that the metapterygial axis rotated outwards from the body wall during evolution^{2,3} (Fig. 4A). Fate maps of cells at the base of a chick wing-bud show that anterior cells remain at the proximal part of the limb, but cells in the middle and posterior regions extend posteriorly and distally as the wing bud grows out (Fig. 4B–D). The relative displacement of these populations is illustrated by the curved red line in Fig. 4C. Support for the idea that *Shh* is involved in this reorientation comes unexpectedly from a recent detailed analysis of *Shh* null mutant mouse embryos, which described the limbs as being 'trapped' within the body wall²².

Our data suggest that the dogfish may represent an important intermediate form in the evolution of tetrapod limbs (Fig. 2b). Although we did not detect lateral fin folds in dogfish, we suggest that an ancestral vertebrate had already been compartmentalized dorso-ventrally with *Engrailed-1* expression ventrally and had lateral fin folds that expressed a single *Tbx4/5* gene (Fig. 2a). This assumes, however, that a lateral fin fold is likely to be primitive. It will be interesting to characterize these features of the body plan in hagfish and lampreys. Our view of the origin of tetrapod limbs also suggests that more attention should be given to mechanisms that inhibit limb development. Many genes that are thought to be involved in limb formation in higher vertebrates, including *Fgf10* and *Hoxd9*, are initially expressed in both limb and inter-limb regions and then 'switch off' in the inter-limb regions. □

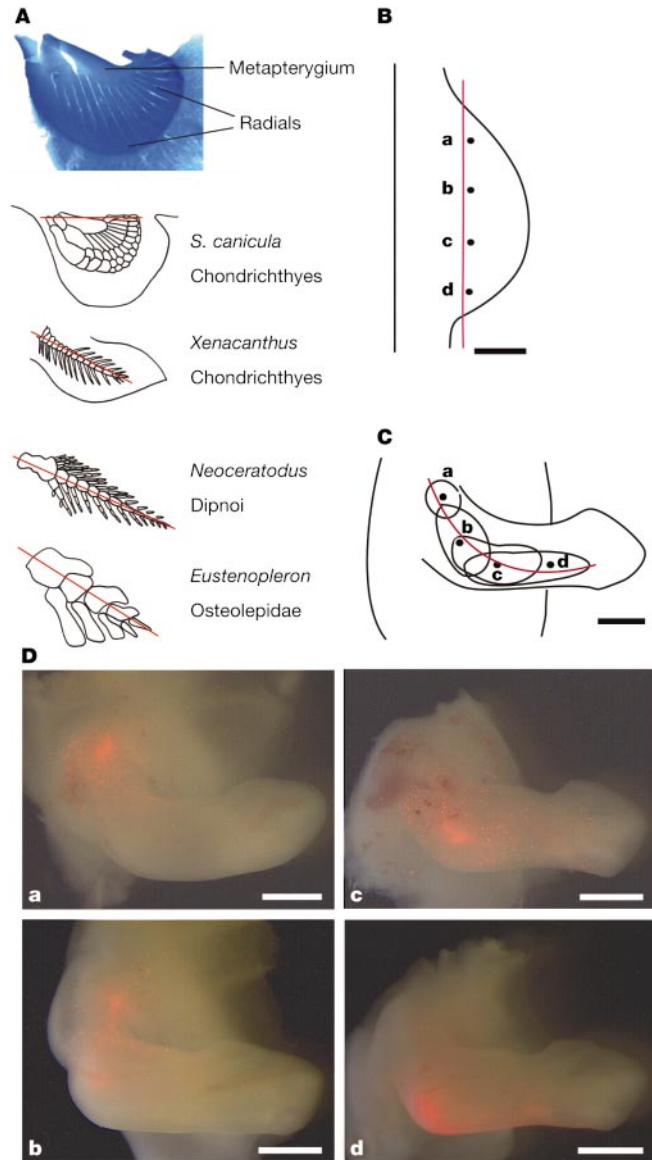


Figure 4 **A**, Series of pectoral appendages comparing the dogfish with other species in which the metapterygial axis is freed from the body wall and forms the main axis of the limb. The red line represents the position of the major axis. In *S. canicula*, the metapterygial stem has retained its original position in the body wall; in the fossils *Xenacanthus* and *Neoceratodus*, the metapterygial stem has become freed from the body wall and forms the principal axis^{3,28}. **B**, Diagram of stage 20 chick wing-bud showing positions at which Dil was injected. Scale bar, 250 μ m. **C**, Map of representative results obtained in chick wing at 96 h for populations of labelled cells. Scale bar, 500 μ m. The relative displacement of cells is illustrated by the red line. **D**, Micrographs showing fate maps of wing buds 96 h after Dil injection at the positions a–d respectively indicated in **B** and **C**. Scale bars 500 μ m.

Methods

Scanning electron microscopy

S. canicula eggs were incubated at 16 °C in sea water and staged according to ref. 8. Embryos were fixed in Peter's fixative (1.25% glutaraldehyde, 1% paraformaldehyde in 0.1 M cacodylate buffer, pH 7.2) at 4 °C. After post-fixation in 1% osmium in cacodylate buffer, specimens were dehydrated in graded ethanol, placed in acetone, critically point-dried, sputter-coated with gold/palladium and viewed on a Hitachi S-4700 field-emission scanning electron microscope.

Identification of *S. canicula* gene homologues

We identified fragments of *S. canicula* *Tbx4* (275 base pairs, bp), *Tbx5* (278 bp), *Engrailed-1* (326 bp), *dHand* (267 bp), *Bmp4* (243 bp) and *Shh* (297 bp) from complementary DNA pools prepared from stage 24–28 embryos⁸ using degenerate primers. The amino-acid sequences used for degenerate primers were: *ScTbx4*, KFCDNKWM and TAFCTHVF; *ScTbx5*, YKFADNKW and TAFCTHVF; *ScEngrailed-1*, WPAWVYCT and MAQGILYNH; *ScdHand*, ECIPNVP and WPQHVA; *ScBmp4*, WIVAPPG and DMVVEG. To avoid

amplification of *Dhh* and *Ihh*, the *ScShh* fragment was obtained by nested PCR. The amino-acid sequences used for degenerate primers were: *ScShh* first PCR, KQFIPNVA and AHIHCSV *ScShh* second, nested PCR, PNYNPDI and GFDWVYYE. The longer *ScShh* (348 bp) fragment was obtained from cDNA pools of stage 27 *S. canicula* embryos by RT-PCR using a degenerate forward primer and a *ScShh*-specific reverse primer (GRYEGKIT and TTCGTAGTAGACCCAGTC). The nucleotide sequences of *ScEn1*, *ScShh*, *ScTbx4*, *ScTbx5*, *ScdHand* and *ScBmp4* cDNA are deposited in the GenBank database under the accession numbers: AF393834–AF393837, AY057890 and AY057891.

In situ hybridization

S. canicula embryos were removed from their egg casings and dissected from the yolk mass. Wholemout *in situ* hybridization on younger *S. canicula* embryos was carried out as previously described²³ and this is based on methods used for other vertebrate embryos²⁴. Older embryos were treated with dimethyl sulphoxide (DMSO) instead of proteinase K treatment by placing them in 2 ml of DMSO/methanol (1:1) on ice until they sank. Then 0.5 ml of 10% Triton X-100 (Sigma) in distilled water was added, and the embryos were incubated for an additional 20 minutes at room temperature^{25,26}. After washing in PBT (1% Tween 20 (Sigma) in PBS), embryos were hybridized with probes as described previously for chick embryos²⁴. Some whole-mount *in situ* samples were embedded in gelatin, and frozen sections were cut.

RT-PCR

RT-PCR was performed as previously described²⁷. The primers used for PCR amplification of *ScShh* (172 bp) were 5'-GAGCTGACAGGCTGATGACAC-3' and 5'-TGGTGATGTCCACAGCTCGGC-3'. The PCR cycle was at 96 °C for 20 seconds, 55 °C for 40 seconds and 72 °C for 1 minute for 32 cycles. Relative levels of transcripts were compared to levels of internal control using 18S ribosomal RNA primers (Ambion). Both *ScShh* and 18S rRNA primers were added into the same reaction solution.

Observation of cartilaginous pattern

S. canicula embryos to be stained for cartilage were fixed in 5% TCA (trichloroacetic acid), stained in 0.1% Alcian blue in 70% acid alcohol, dehydrated in ethanol and cleared in methyl salicylate.

Dil labelling

Dil (1,1-dioctadecyl-3,3,3'-tetramethylindo-carbocyanine perchloride; Molecular Probes; 3 mg ml⁻¹ in DMSO) was injected into chick wing-bud using a micropipette to label a small group of cells. Embryos were then incubated for 96 h and fixed in 4% paraformaldehyde in PBS. The average size of the initial Dil injected dot was 40–50 µm.

Received 2 July; accepted 17 December 2001.

1. Thacher, J. K. Median and paired fins, a contribution to the history of vertebrate limbs. *Trans. Conn. Acad.* **3**, 281–310 (1877).
2. Jarvik, E. in *Basic Structure and Evolution of Vertebrates* 109–131 (Academic, London, 1980).
3. Moy-Thomas, J. A. The evolution of the pectoral fins of fishes and the tetrapod forelimb. *School Sci. Rev.* **36**, 592–599 (1936).
4. Coates, M. I. The origin of vertebrate limbs. *Development* (1994 Suppl.), 169–180 (1994).
5. Shu, D.-G. *et al.* Lower Cambrian vertebrates from South China. *Nature* **402**, 42–46 (1999).
6. Neyt, C. *et al.* Evolutionary origins of vertebrate appendicular muscle. *Nature* **408**, 82–86 (2000).
7. Balfour, F. M. The development of elasmobranch fishes. *J. Anat. Physiol. Lond.* **11**, 128–172 (1876).
8. Ballard, W. W., Mellinger, J. & Lechenault, H. A series of normal stages for development of *Scyliorhinus canicula*, the lesser spotted dogfish (*Chondrichthyes: Scyliorhinidae*). *J. Exp. Zool.* **267**, 318–336 (1993).
9. Altäbef, M., Clarke, J. D. & Tickle, C. Dorsal-ventral ectodermal compartments and origin of apical ectodermal ridge in developing chick limb. *Development* **124**, 4547–4556 (1997).
10. Tanaka, M. *et al.* Apical ectodermal ridge induction by the transplantation of En-1-overexpressing ectoderm in chick limb bud. *Dev. Growth Differ.* **40**, 423–429 (1998).
11. Tabin, C. & Laufer, E. *Hox* genes and serial homology. *Nature* **361**, 692–693 (1993).
12. Coates, M. I. *Hox* genes, fin folds and symmetry. *Nature* **364**, 195–196 (1993).
13. Tamura, K. *et al.* Evolutionary aspects of positioning and identification of vertebrate limbs. *J. Anat.* **199**, 195–204 (2001).
14. Ruvinsky, I., Silver, L. M. & Gibson-Brown, J. J. Phylogenetic analysis of T-box genes demonstrates the importance of amphioxus for understanding evolution of the vertebrate genome. *Genetics* **156**, 1249–1257 (2000).
15. Balinsky, B. I. Das Extremitätenseitenfeld, seine Ausdehnung und Beschaffenheit. *Roux Arch. Dev. Biol.* **130**, 704–736 (1933).
16. Cohn, M. J., Izpisua-Belmonte, J. C., Abud, H., Heath, J. K. & Tickle, C. Fibroblast growth factors induce additional limb development from the flank of chick embryo. *Cell* **80**, 739–746 (1995).
17. Tanaka, M. *et al.* Distribution of polarizing activity and potential for limb formation in mouse and chick embryos and possible relationship to polydactyly. *Development* **127**, 4011–4021 (2000).
18. Riddle, R. D., Johnson, R. L., Laufer, E. & Tabin, C. *Sonic hedgehog* mediates the polarizing activity of the ZPA. *Cell* **75**, 1401–1416 (1993).
19. Ekker, S. C. *et al.* Patterning activities of vertebrate hedgehog proteins in the developing eye and brain. *Curr. Biol.* **5**, 44–55 (1995).
20. Cohn, M. J. Giving limbs a hand. *Nature* **406**, 953–954 (2000).
21. Tümpel, S. *et al.* Antero-posterior signaling in vertebrate limb development and stripes of *Tbx3* expression. *Dev. Biol.* (submitted).
22. Kraus, P., Fraidenraich, D. & Loomis, C. A. Some distal limb structures develop in mice lacking Sonic hedgehog signaling. *Mech. Dev.* **100**, 45–58 (2001).

23. Mazan, S., Jaillard, D., Baratte, B. & Janvier, P. *Otx1* gene-controlled morphogenesis of the horizontal semicircular canal and the origin of the gnathostome characteristics. *Evol. Dev.* **2**, 186–193 (2000).
24. Wilkinson, D. G. *In Situ Hybridization: A Practical Approach* 75–83 (IRL Press/Oxford Univ. Press, Oxford, 1992).
25. Kuratani, S., Ueki, T., Aizawa, S. & Hirano, S. Peripheral development of cranial nerves in a cyclostome, *Lampetra japonica*: morphological distribution of nerve branches and the vertebrate body plan. *J. Comp. Neurol.* **384**, 482–500 (1997).
26. Schlosser, G. & Roth, G. Evolution of nerve development in frogs. I. The development of the peripheral nervous system in *Discoglossus pictus* (Discoglossidae). *Brain Behav. Evol.* **50**, 61–93 (1997).
27. Münsterberg, A. E., Kitajewski, J., Bumcrot, D. A., McMahon, A. P. & Lassar, A. B. Combinatorial signaling by Sonic hedgehog and Wnt family members induces myogenic bHLH gene expression in the somite. *Genes Dev.* **9**, 2911–2922 (1995).
28. Coates, M. I. Limb evolution. Fish fins or tetrapod limbs—a simple twist of fate? *Curr. Biol.* **5**, 844–848 (1995).

Supplementary Information accompanies the paper on Nature's website (<http://www.nature.com>).

Acknowledgements

We are grateful to A. Wells for his assistance in maintenance of *S. canicula* embryos, S. Kuratani for information about *S. canicula* developmental studies before publication, S. Mazan for technical advice and *ScOtx1* and *ScOtx2* cDNA as positive control probes for establishing *in situ* hybridization methods and N. Helps for DNA sequencing. M.T. is supported by JSPS Postdoctoral Fellowships for Research Abroad, JSPS Research Fellowships for Young Scientists and the Inoue Research Award for Young Scientists. A.M. is supported by a Wellcome Trust research Career Development Award. C.T. is Foulerton Research Professor of The Royal Society.

Correspondence and requests for materials should be addressed to M.T. (e-mail: m.tanaka@dundee.ac.uk).

The cost of inbreeding in *Arabidopsis*

Carlos D. Bustamante[†], Rasmus Nielsen[‡], Stanley A. Sawyer[§], Kenneth M. Olsen^{||}, Michael D. Purugganan^{||} & Daniel L. Hartl^{*}

^{*} Department of Organismic and Evolutionary Biology, Harvard University, 16 Divinity Avenue, Cambridge, Massachusetts 02138, USA
[‡] Department of Biometrics, Cornell University, Ithaca, New York 14853-2801, USA
[§] Department of Mathematics, Washington University, St Louis, Missouri 63130, USA
^{||} Department of Genetics, North Carolina State University, Raleigh, North Carolina 27695-7614, USA

Population geneticists have long sought to estimate the distribution of selection intensities among genes of diverse function across the genome. Only recently have DNA sequencing and analytical techniques converged to make this possible. Important advances have come from comparing genetic variation within species (polymorphism) with fixed differences between species (divergence)^{1,2}. These approaches have been used to examine individual genes for evidence of selection. Here we use the fact that the time since species divergence allows combination of data across genes. In a comparison of amino-acid replacements among species of the mustard weed *Arabidopsis* with those among species of the fruitfly *Drosophila*, we find evidence for predominantly beneficial gene substitutions in *Drosophila* but predominantly detrimental substitutions in *Arabidopsis*. We attribute this difference to the *Arabidopsis* mating system of partial self-fertilization, which corroborates a prediction of population genetics theory^{3–6} that species with a high frequency of inbreeding are less efficient in eliminating deleterious mutations owing to their reduced effective population size.

We analysed *Arabidopsis* data for 12 genes of diverse function for

[†] Present address: Department of Statistics, University of Oxford, Oxford OX1 3TG, UK.